JGR Solid Earth

RESEARCH ARTICLE
10.1029/2020JB020642

Key points:

- The aim of this paper is to contribute to understand the short-period oscillations of effusion rate in eruptions
- A model is proposed to explain the evolution of effusion rate due to pressure oscillations in the volcanic conduit, embedded in a viscoelastic medium
- For fissures the viscoelastic rheology entails a remarkable increase in oscillation amplitude of flow rate with respect to the elastic case and a time delay in flow rate oscillation with respect to overpressure oscillation

Correspondence to:
A. Piombo,
antonello.piombo@unibo.it

Citation:
Piombo, A., & Dragoni, M. (2021). Effusion rate from a volcanic conduit subject to pressure oscillations in a viscoelastic medium. *Journal of Geophysical Research: Solid Earth*, *126*, e2020JB020642. https://doi.org/10.1029/2020JB020642

Received 24 JUL 2020
Accepted 23 NOV 2020

Effusion Rate From a Volcanic Conduit Subject to Pressure Oscillations in a Viscoelastic Medium

Antonello Piombo[1], and Michele Dragoni[1]

[1]Dipartimento di Fisica e Astronomia "Augusto Righi", Alma Mater Studiorum - Università di Bologna, Bologna, Italy

Abstract Effusion rate in basaltic eruptions typically depends on time: there is an initial, relatively fast increase followed by a much slower decrease until the eruption vanishes; in addition, changes are observed in the effusion rate having durations much shorter than the total duration of the eruption. For an effusive eruption, we calculate the deformation of the volcanic conduit due to short-term pressure oscillations. The model considers an elliptical conduit embedded in a viscoelastic medium, described by a Maxwell body. As a consequence of pressure oscillations, the semi axes of the conduit are quasi periodic functions of time with the same period as pressure. For volcanic fissures the viscoelastic rheology entails a remarkable increase in oscillation amplitude of flow rate with respect to the elastic case and a time delay in flow rate oscillation with respect to overpressure oscillation. For a given value of overpressure amplitude, this effect is controlled by the conduit eccentricity and the ratio between overpressure period and Maxwell time; for larger values of this ratio and/or for eccentricity values closer to unity, flow rate oscillates around a value larger than its initial value and can vary from 5% to 30% with respect to it. The model can approximate the in-situ observations of short-time fluctuations of flow rate during the 2018 eruption of Kīlauea Volcano.

1. Introduction

The evaluation of volcanic hazard associated with lava flows depends in large part on lava flow forecasting accuracy. For effusive eruptions, the most important questions are how rapidly will flows advance, how large an area will be covered by lava, and how far will the furthest lavas flow. The effusion rate of lava from an eruption vent is the primary quantity controlling the advance rate, length, and coverage of lava flows. For this reason much effort is devoted to the evaluation of this quantity (e.g., Calvari & Pinkerton, 1999).

Effusion rate in basaltic eruptions typically depends on time: there is an initial, relatively fast increase followed by a much slower decrease until the eruption vanishes (e.g., Del Negro et al., 2013; Vicari et al., 2011). The observed dependence on time of effusion rate has been explained by the decrease of pressure gradient in the volcanic conduit due to progressive emptying of the magma chamber (Wadge, 1981), and by the mechanical erosion of the conduit wall produced by magma flow (Piombo et al., 2016).

During effusive eruptions, Lautze et al. (2004) observed changes in the effusion rate having durations much shorter than the total duration of the eruption. Effusion rate and degassing data show variations occurring on timescales of hours to months (e.g., Voight et al., 1999) due to fluctuations in the supply rate from the magma chamber and/or conduit processes that interfere with an approximately constant supply rate: flow oscillations may result from temperature changes in a fluid with a temperature-dependent viscosity (Whitehead & Helfrich, 1991), small chamber overpressures (Woods & Koyaguchi, 1994), rapid changes in the width of the conduit outlet by viscous flow of wall rocks (Ida, 1996), the dependence of viscosity on the volatile content of magma (Wylie et al., 1999), high frequency pressure fluctuations due to the ascending magma column surrounded by an annulus of compressible foam (Jellinek & Bercovici, 2011). Ripepe et al. (2002) indicated that mass flow may proceed in a pulsatory manner. The positive correlation of degassing and explosive activity suggests that they are due to pressure changes in the conduit associated with changes in volatile content (Gonnermann & Manga, 2013; Sparks, 2003). This pulsatory style was observed during the 2018 highly destructive eruption occurred on the lower flank of Kīlauea Volcano, Hawaii: the eruption rate exhibited cyclic behavior on multiple time scales (Patrick et al., 2019) and, in addition, the main flow was exceptionally well monitored (Neal et al., 2019). Patrick et al. (2019) concluded that short-term fluctuations were controlled by changes in outgassing efficiency of the lava at shallow depths, while long-term fluctuations were controlled by pressure transients due to the summit caldera collapse of Kīlauea Volcano.

In volcanic areas, rocks near magmatic sources are considerably heated, producing effective viscosities orders of magnitude lower than typical crustal values. Because of the relatively high temperatures in these areas, observed deformation can be more properly modeled by a viscoelastic rheology (e.g., Bonafede et al., 1986; Dragoni & Magnanensi, 1989; Filippucci et al., 2013; Folch et al., 2000; Newman et al., 2001; Piombo et al., 2007; Tallarico et al., 2011).

In general, volcanic conduits have irregular cross-sections (e.g., Calvari & Pinkerton, 1999). Dynamical and thermal aspects of lava conduits were studied assuming cylindrical shapes with circular and elliptical cross-sections (e.g., Dragoni et al., 2002; Dragoni & Santini, 2007; Dragoni & Tallarico, 2008; Sakimoto & Zuber, 1998).

Dragoni and Tallarico (2019) investigated the effects of pressure oscillations in a volcanic conduit filled by magma. Considering a cylindrical conduit with elliptical cross-section, embedded in an elastic medium, they showed that deformation of the conduit wall can produce oscillations in magma flow rate, hence in effusion rate at the volcanic vent; they found that the amplitude of flow rate oscillations is remarkable only in the case of long and narrow volcanic fissures.

In the present paper, we study pressure oscillations in a volcanic conduit embedded in a viscoelastic medium. Due to the high temperatures induced by magma in the surrounding rocks, a viscoelastic rheology is more appropriate to describe their mechanical behavior. In particular, we assume that conduit deformation is controlled by the rheological properties in the proximity of the conduit itself and represent the medium as a homogeneous and isotropic Maxwell body.

The aim of the present paper is to calculate the changes in the area of the conduit cross section due to pressure oscillations and the ensuing changes in magma flow rate and in the effusion rate at the Earth's surface.

2. The Model

We assume that the conduit is a right cylinder filled by magma and embedded in an isotropic viscoelastic medium. The medium is a Maxwell body with Lamé constants λ and μ and viscosity η. The axis of the conduit is the z-axis of a Cartesian coordinate system. We assume that the conduit cross-section is an ellipse with semi-major axis a and semi-minor axis b. The equation of the conduit wall is then

$$\frac{x^2}{a^2} + \frac{y^2}{b^2} = 1 \tag{1}$$

with focal distance

$$c = \sqrt{a^2 - b^2} \tag{2}$$

and eccentricity

$$\epsilon = \frac{c}{a} \tag{3}$$

In order to solve the problem, it is appropriate to use elliptic cylindrical coordinates (α, β, z), with

$$x = c\cosh\alpha\cos\beta, \qquad y = c\sinh\alpha\sin\beta, \qquad z = z \tag{4}$$

where $\alpha \geq 0$ and $0 \leq \beta < 2\pi$. In these coordinates, the conduit wall is defined by the equation

$$\alpha = \alpha_1 \tag{5}$$

where

$$\alpha_1 = \operatorname{arccosh}\frac{a}{c} \tag{6}$$

For the sake of simplicity, we assume that the conduit is embedded in an unbounded medium, that is reasonable if we consider a conduit stretch that is not too close to the eruption vent.

We suppose that at $t = 0$, an overpressure develops in the conduit, oscillating according to the equation

$$p(t) = p_0 H(t) \sin \omega t \tag{7}$$

where $H(t)$ is the Heaviside function, p_0 is the amplitude, and ω is the frequency of oscillations. If τ_0 is the period, then

$$\omega = \frac{2\pi}{\tau_0} \tag{8}$$

If pressure changes are slow and strain is small, the quasistatic, small-strain theory can be applied. The equilibrium equation is

$$\nabla \cdot \boldsymbol{\sigma} = 0 \tag{9}$$

where $\boldsymbol{\sigma}$ is the stress produced by the overpressure $p(t)$. The axial symmetry of the system suggests that the u_α and u_β components of displacement depend only on α and β. As to the u_z component, we assume that it vanishes, because the vertical deformation produced by magma drag at the conduit wall is negligible compared to the horizontal deformation due to the lava pressure and its change. This is a state of plane strain (e.g., Landau & Lifshits, 1970), implying that no quantity depends on z. Accordingly, the $\sigma_{\alpha z}$ and $\sigma_{\beta z}$ components of stress vanish.

The solution for a homogeneous elastic medium surrounding the volcanic conduit has been given in Dragoni and Tallarico (2019). In the case of a Maxwell viscoelastic medium, deformation of the conduit wall is controlled by the rheological parameters λ, μ, and η, according to the constitutive equation

$$\dot{\boldsymbol{\sigma}} + \frac{\mu}{\eta}\left[\boldsymbol{\sigma} - \frac{1}{3}(Tr\boldsymbol{\sigma})\boldsymbol{I}\right] = \lambda(Tr\dot{\boldsymbol{e}})\boldsymbol{I} + 2\mu\dot{\boldsymbol{e}} \tag{10}$$

where $\boldsymbol{e}$ is the strain tensor and dots indicate differentiation with respect to time. This equation expresses the fact that viscoelastic behavior of rocks mainly concerns deviatoric stress (e.g., Peltier, 1974).

We assume a stationary temperature field around the conduit. If χ is the thermal diffusivity of the medium, this condition is reached at a distance L from the conduit wall after a time

$$\tau \simeq \frac{L^2}{4\chi} \tag{11}$$

For $\chi \simeq 10^{-6}$ m^2/s, steady state is achieved after less than 3 days from the eruption beginning inside a 1-m-thick layer around the conduit.

The three rheological parameters λ, μ, and η are temperature dependent. According to Dragoni and Tallarico (2008), temperature T around a cylindrical conduit with elliptical cross section is a linearly decreasing function of the distance α from the conduit axis, given by

$$T(\alpha) = T_1 - (T_1 - T_2)\frac{\alpha - \alpha_1}{\alpha_2 - \alpha_1} \tag{12}$$

where T_1 is the wall temperature and T_2 is the ambient temperature at distance $\alpha_2 \gg \alpha_1$.

The Lamé constants λ and μ are slowly decreasing functions of temperature (e.g., Ji et al., 2010), that can be approximated as

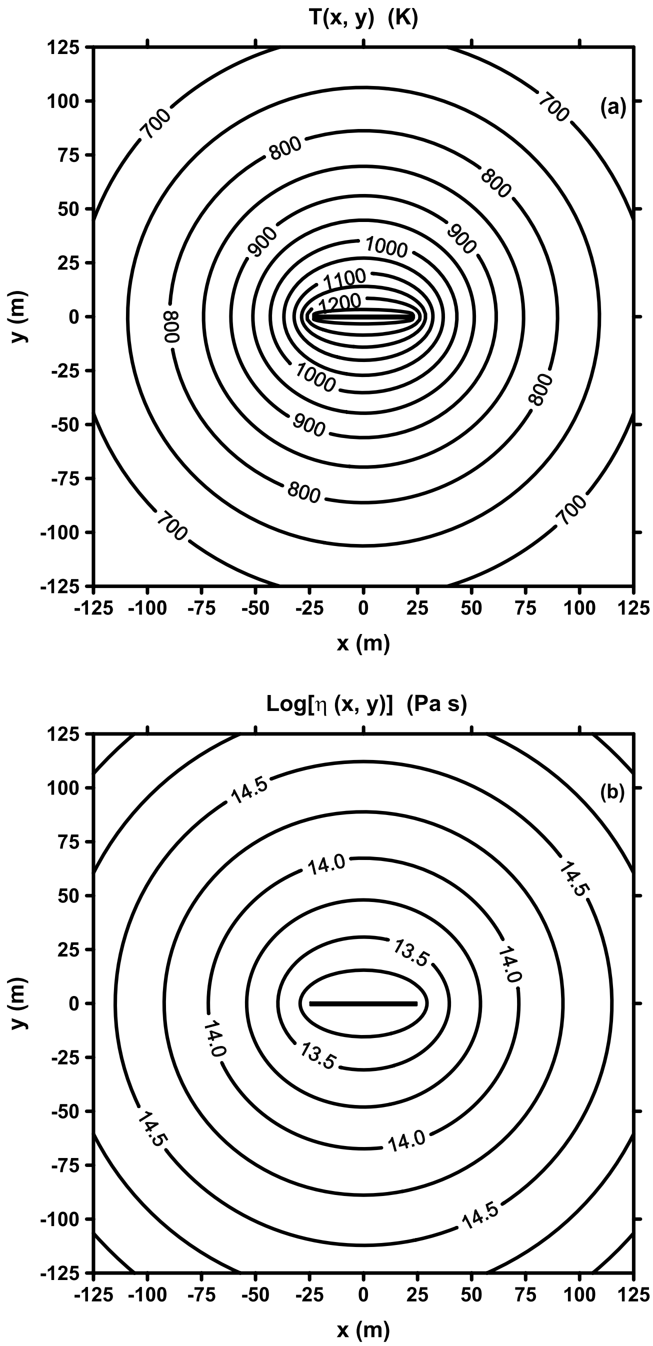

Figure 1. Temperature $T(x, y)$ (a) and the corresponding viscosity field $\eta(x, y)$ (b) for a choice of values of parameters (Table 1) and $a = 25$ m, $b = 1$ m ($\epsilon \simeq 0.9992$)

$$\lambda(T) = \lambda_2 - k(T - T_2) \tag{13}$$

where $\lambda_2 = \lambda(T_2)$ and k is a constant. A similar equation can be written for μ. The dependence of viscosity on temperature is given by the Arrhenius formula

$$\eta(T) = A_D e^{\frac{E}{RT}} \tag{14}$$

where A_D is the Dorn parameter, E is the activation energy and R is the gas constant (e.g., Ranalli, 1995).

Figure 1 shows a contour graph of temperature (a) and viscosity (b) as functions of x and y for $b = 1$ m and $a = 25$ m and for a choice of values of parameters (Table 1). At the conduit wall viscosity is about 10^{13} Pa s. We note that temperature is slowly decreasing away from the conduit wall.

Introducing (12) into (13) and (14), we can draw graphs of the ratios λ/λ_1 (or μ/μ_1) and η/η_1 as functions of α/α_1 (Figure 2), where the subscript 1 indicates values at the conduit wall. It can be seen that the three parameters are slowly increasing away from the conduit wall.

We can reasonably assume that conduit deformation is mostly affected by the rheological properties in the vicinity of the conduit itself. In this region, according to the previous considerations, we may assume that the rheological parameters have constant values, corresponding to temperature T_1: then we set $\lambda = \lambda_1$, $\mu = \mu_1$, and $\eta = \eta_1$.

Considering the Lamé constants and the viscosity as uniform in space has the advantage that we can apply the correspondence theorem to the elastic solution and can easily obtain the solution of the viscoelastic problem (e.g., Fung, 1965).

3. Elastic Solution

The displacement has components u_α and u_β and the nonvanishing components of stress are $\sigma_{\alpha\alpha}$, $\sigma_{\beta\beta}$, $\sigma_{\alpha\beta}$, and σ_{zz}. The boundary conditions are given by continuity of traction at the conduit wall, that is,

$$\sigma_{\alpha\alpha}(\alpha_1, \beta) = -p, \qquad \sigma_{\alpha\beta}(\alpha_1, \beta) = 0 \tag{15}$$

From Dragoni and Tallarico (2019), the displacement components are

$$u_\alpha(\alpha, \beta, t) = \frac{c}{4} \frac{f_1(t)\cosh 2\alpha_1 + f_2(t)e^{-2\alpha} - f_3(t)\cos 2\beta}{\sqrt{\sinh^2 \alpha + \cos^2 \beta}} \tag{16}$$

$$u_\beta(\alpha, \beta, t) = \frac{c}{4} \frac{f_2(t)\sin 2\beta}{\sqrt{\sinh^2 \alpha + \cos^2 \beta}} \tag{17}$$

where

$$f_1(t) = \frac{p(t)}{\mu} \tag{18}$$

Table 1
Values of Parameters, Considered Fixed in the Paper

Symbol	Quantity	Value
A_D	Dorn parameter	9×10^{10} Pa s
E	Activation energy	5×10^{4} J mol^{-1}
k	Coefficient in (13)	20 MPa K^{-1}
p_0	Pressure oscillation amplitude	10^5 Pa
R	Gas constant	8.314 J K^{-1} mol^{-1}
T_1	Temperature at the conduit wall	1273 K
T_2	Ambient temperature	293 K
α_2	Distance of boundary at $T = T_2$	100 α_1
γ	Body force intensity	10^2 Pa m^{-1}
η_m	Magma viscosity	10^2 Pa s
λ, μ	Lamé constants	10 GPa
λ_1, μ_1	Lamé constants at $\alpha = \alpha_1$	10 GPa
λ_2, μ_2	Lamé constants at $\alpha = \alpha_2$	30 GPa

$$f_2(t) = \frac{p(t)}{\lambda + \mu} \tag{19}$$

$$f_3(t) = \frac{\lambda + 2\mu}{\lambda + \mu}\frac{p(t)}{\mu} \tag{20}$$

Both components u_α and u_β are periodic in β with period π. For large eccentricities ($\epsilon > 0.9$) $u_\beta \ll u_\alpha$, so the wall displacement depends mainly on u_α.

4. Viscoelastic Solution

The viscoelastic solution for displacement and stress in the medium can be obtained from the elastic solution by application of the correspondence theorem (e.g., Christensen, 1982; Fung, 1965). For a homogeneous and isotropic medium, the application of the correspondence theorem requires the substitution in the elastic solution of the Lamé constants λ and μ with complex expressions:

$$\lambda \to \tilde{\lambda}(s) \, , \qquad \mu \to \tilde{\mu}(s), \tag{21}$$

where s is the complex variable conjugate to time. Various kinds of rheologies are possible for a viscoelastic medium; the specific functions $\tilde{\lambda}$ and $\tilde{\mu}$ depend on the rheology considered. In addition, one must substitute the source function $F(t)$ with its Laplace transform:

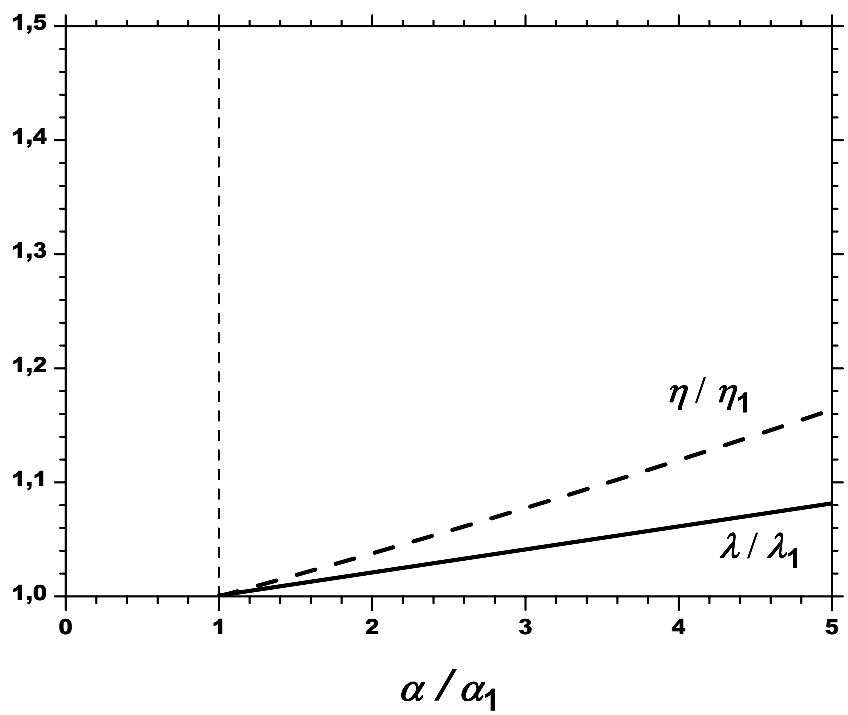

Figure 2. Lamé parameter λ (or μ) and viscosity η as functions of distance α from the conduit axis (values of relevant quantities as in Table 1). Subscript 1 indicates values at the conduit wall

$$F(t) \to \tilde{F}(s). \tag{22}$$

We assume that the medium deforms viscoelastically with respect to shear stresses but elastically with respect to normal stresses. Assuming that the viscoelastic behavior is that of a Maxwell body, described by Equation 10, in the expressions of displacement field 16 and 17, given by Dragoni and Tallarico (2019), we make the substitutions

$$p(t) \to \tilde{p}(s) = p_0 \frac{\omega}{s^2 + \omega^2} \tag{23}$$

$$\mu \to \tilde{\mu}(s) = \frac{\mu s}{s + \mu\eta} \tag{24}$$

$$\lambda \to \tilde{\lambda}(s) = \lambda + \frac{2}{3}\mu - \frac{2}{3}\tilde{\mu}(s) \tag{25}$$

and we obtain the expressions for the Laplace transforms $\tilde{u}_\alpha(\alpha,\beta,s)$ and $\tilde{u}_\beta(\alpha,\beta,s)$ of viscoelastic displacements.

According to the correspondence theorem, we obtain the viscoelastic solution by inverting the Laplace transforms $\tilde{u}_\alpha$ and $\tilde{u}_\beta$, which gives

$$U_\alpha(\alpha,\beta,t) = \frac{c}{4}\frac{F_1(t)\cosh 2\alpha_1 + F_2(t)e^{-2\alpha} - F_3(t)\cos 2\beta}{\sqrt{\sinh^2\alpha + \cos^2\beta}} \tag{26}$$

$$U_\beta(\alpha,\beta,t) = \frac{c}{4}F_2(t)\frac{\sin 2\beta}{\sqrt{\sinh^2\alpha + \cos^2\beta}} \tag{27}$$

where

$$F_1(t) = \frac{p_0}{\mu}\left(\sin\omega t - \frac{1}{\omega\tau_1}\cos\omega t + \frac{1}{\omega\tau_1}\right) \tag{28}$$

$$\begin{aligned} F_2(t) = {} & 3\frac{p_0}{3\lambda + 2\mu}\frac{1}{1 + \omega^2\tau_2^2} \times \\ & \left[(1 + \omega^2\tau_1\tau_2)\sin\omega t - \frac{\mu}{3\lambda + 2\mu}\omega\tau_1\cos\omega t + \frac{\mu}{3\lambda + 2\mu}\omega\tau_1 e^{-\frac{t}{\tau_2}}\right] \end{aligned} \tag{29}$$

$$\begin{aligned} F_3(t) = {} & \frac{p_0}{\mu}\frac{1}{\omega\tau_1}\frac{1}{1 + \omega^2\tau_2^2} \times \\ & \left\{\left[\frac{3\lambda + 5\mu}{3\lambda + 2\mu} + 9\frac{(\lambda + \mu)(\lambda + 2\mu)}{(3\lambda + 2\mu)^2}\omega^2\tau_1^2\right]\omega\tau_1\sin\omega t\right. \\ & -\left[3\frac{3\lambda^2 + 6\lambda\mu + 4\mu^2}{(3\lambda + 2\mu)^2}\omega^2\tau_1^2 + 1\right]\cos\omega t \\ & \left.+(\frac{3\mu^2}{(3\lambda + 2\mu)^2}\omega^2\tau_1^2 e^{-\frac{t}{\tau_2}} + 1 + \omega^2\tau_2^2\right\} \end{aligned} \tag{30}$$

and

$$\tau_1 = \frac{\eta}{\mu} \tag{31}$$

$$\tau_2 = 3\frac{\lambda + \mu}{3\lambda + 2\mu}\tau_1 \tag{32}$$

For very large values of viscosity the solution tends to elastic one:

$$F_i(t) \overset{\eta\to+\infty}{\to} f_i(t) \ , \ i = 1,2,3 \tag{33}$$

We note that the functions f_i of the elastic case are periodic with the same period τ_0 of overpressure $p(t)$, while only F_1 has exactly this property in the viscoelastic case; moreover, if τ_1 and τ_2 are smaller than or equal to τ_0, the functions F_2 and F_3 are with good approximation periodic with a period equal to the forcing oscillation, because the aperiodic terms vanish exponentially with time.

The deformation of the conduit wall is described in terms of the α-component of displacement calculated at $\alpha = \alpha_1$, that is,

$$\begin{aligned} U_\alpha(\alpha_1,\beta,t) = & \frac{1}{4}\frac{1}{\sqrt{(a^2-b^2)\cos^2\beta + b^2}} \times \\ & \left[(a^2+b^2)F_1(t) + (a-b)^2F_2(t)\right) \\ & \left(-(a^2-b^2)F_3(t)\cos 2\beta\right] \end{aligned} \tag{34}$$

5. Effect on Flow Rate

We assume that the magma flowing in the conduit is a homogeneous, isotropic and incompressible Newtonian liquid with viscosity η_m. We consider a laminar, steady-state flow, so that the magma flow rate in the undeformed conduit is (Dragoni & Santini, 2007)

$$Q_0 = \frac{\pi}{4}\frac{\gamma}{\eta_m}\frac{a^3b^3}{a^2+b^2} \tag{35}$$

where the body force intensity γ is considered a constant. As shown in Dragoni and Tallarico (2019), the deformed cross section is still an ellipse to a very good approximation. It is the same in the present model, with semi-major and semi-minor axes

$$\begin{aligned} A(t) &= a + U_\alpha(\alpha_1,0,t) \\ &= a + \frac{1}{4}\frac{1}{a}\left[(a^2+b^2)F_1(t) + (a-b)^2F_2(t) - (a^2-b^2)F_3(t)\right] \end{aligned} \tag{36}$$

$$\begin{aligned} B(t) &= b + U_\alpha\left(\alpha_1,\frac{\pi}{2},t\right) \\ &= b + \frac{1}{4}\frac{1}{b}\left[(a^2+b^2)F_1(t) + (a-b)^2F_2(t) + (a^2-b^2)F_3(t)\right] \end{aligned} \tag{37}$$

At any time $t \geq 0$, the flow rate is

$$Q(t) = \frac{\pi}{4}\frac{\gamma}{\eta_m}\frac{A(t)^3B(t)^3}{A(t)^2+B(t)^2} \tag{38}$$

with a ratio

$$\frac{Q(t)}{Q_0} = \frac{a^2 + b^2}{a^3 b^3} \frac{A(t)^3 B(t)^3}{A(t)^2 + B(t)^2} \tag{39}$$

6. Volcanic Fissure Approximation

For a volcanic conduit with elliptical cross-section, embedded in an elastic medium, Dragoni and Tallarico (2019) found that the amplitude of flow rate oscillations is remarkable only in the case of long and narrow volcanic fissures. In this case, the semi-axes can be approximated ($b \ll a$) by

$$A^{\mathrm{el.}}(t) \simeq a \tag{40}$$

$$B^{\mathrm{el.}}(t) \simeq b\left(1 + \frac{1}{2}\frac{\lambda + 2\mu}{\lambda + \mu}\frac{p_0}{\mu}\frac{1}{1-\epsilon^2}\sin\omega t\right) \tag{41}$$

and, for $\lambda = \mu$,

$$B^{\mathrm{el.}}(t) \simeq b\left(1 + \frac{3}{4}\frac{p_0}{\mu}\frac{1}{1-\epsilon^2}\sin\omega t\right) \tag{42}$$

For a conduit embedded in a viscoelastic medium, the semi-axes $A(t)$ and $B(t)$, and so flow rate $Q(t)$, depend mainly on the amplitude p_0 and the period τ_0 of overpressure, the Maxwell relaxation time τ_1 (and τ_2) and the fissure eccentricity ϵ. From 36, 37, 28–30, and 32, if $b \ll a$ and $\lambda = \mu$, the semi-axes of conduit are approximated by

$$A(t) \simeq a \tag{43}$$

$$B(t) \simeq b\left\{1 + \frac{1}{4}\frac{p_0}{\mu}\frac{1}{1-\epsilon^2}\left[c_1(1-\cos\omega t) + c_2\left(\cos\omega t - e^{-\frac{5}{6}\frac{t}{\tau_1}}\right) + c_3\sin\omega t\right]\right\} \tag{44}$$

where the coefficients c_i are functions of τ_0 and τ_1

$$c_1 = \frac{2}{\omega\tau_1} \tag{45}$$

$$c_2 = -6\frac{\omega\tau_1}{25 + 36\,\omega^2\tau_1^2} \tag{46}$$

$$c_3 = 3 + \frac{5}{25 + 36\,\omega^2\tau_1^2} \tag{47}$$

Figure 3 shows the coefficients c_i as functions of ratio of the Maxwell time τ_1 to the overpressure period τ_0. We note that all functions are constant for $\tau_1/\tau_0 > 10$: $c_3 \simeq 3$ and $c_1 \simeq c_2 \simeq 0$. For $\tau_1/\tau_0 \leq 10$, c_1 varies with this ratio, while c_2 and c_3 remain about constant. Comparing 41 with 44, from Figure 3 we deduce that only for $\tau_1/\tau_0 \leq 10$ the viscoelastic rheology differentiates from the elastic case and this characteristic is more evident as τ_1/τ_0 is smaller. This is more evident if we consider the maximum and minimum values of the semi-minor axis: B reaches its maximum value

$$B_{\max} \simeq b\left\{1 + \frac{1}{4\pi}\frac{p_0}{\mu}\frac{1}{1-\epsilon^2}\frac{\tau_0}{\tau_1}\left[1 + \sqrt{1 + 9\pi^2\left(\frac{\tau_1}{\tau_0}\right)^2}\right]\right\} \tag{48}$$

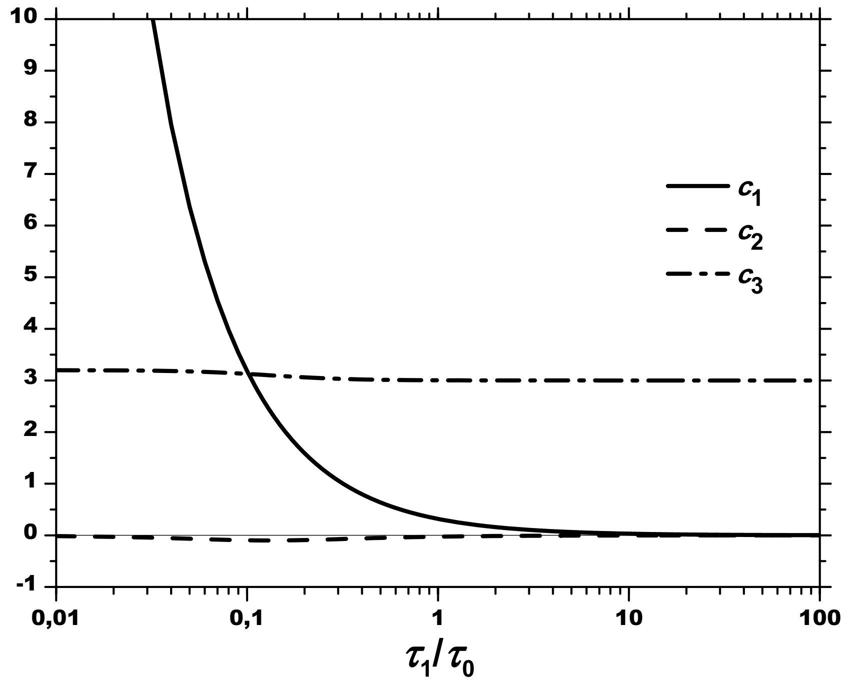

Figure 3. The coefficients c_i as functions of τ_1/τ_0

at

$$t_{\max} \simeq \frac{\tau_0}{2\pi}\left[\pi - \arctan\left(3\pi\frac{\tau_1}{\tau_0}\right)\right] \tag{49}$$

while it reaches its minimum value

$$B_{\min} \simeq b\left\{1 + \frac{1}{4\pi}\frac{p_0}{\mu}\frac{1}{1-\epsilon^2}\frac{\tau_0}{\tau_1}\left[1 - \sqrt{1 + 9\pi^2\left(\frac{\tau_1}{\tau_0}\right)^2}\right]\right\} \tag{50}$$

at

$$t_{\min} \simeq \frac{\tau_0}{2\pi}\left[2\pi - \arctan\left(3\pi\frac{\tau_1}{\tau_0}\right)\right] \tag{51}$$

where $t_{\max}$ and $t_{\min}$ depend only on τ_0 and τ_1. In the viscoelastic case, for given values of overpressure amplitude and rigidity, the oscillation of semi-minor axis is more remarkable for eccentricity values closer to unity and if the overpressure period is larger than the Maxwell relaxation time; furthermore, when τ_1/τ_0 decreases $B_{\max}$ increases and $|B_{\min}|$ decreases, while $t_{\max}$ and $t_{\min}$ are delayed with respect to elastic case and approach $\tau_0/2$ and τ_0, respectively.

From 44–47 and 48 we note that the oscillation amplitude of $B(t)$ is controlled by the parameter

$$\xi = \frac{p_0}{\mu}\frac{1}{1-\epsilon^2}\frac{\tau_0}{\tau_1} \tag{52}$$

$B(t)$ oscillates around the value

$$\frac{B_{\max} + B_{\min}}{2} \simeq b + \frac{1}{4\pi}\xi \tag{53}$$

Table 2
The Four Cases Illustrated in Figures 6 and 7

	Case 1	Case 2	Case 3	Case 4
a	25 m	25 m	50 m	50 m
b	1 m	1 m	1 m	1 m
ϵ	0.9992	0.9992	0.9998	0.9998
τ_0	12 h	6 h	6 h	1 h
ξ	0.3	0.1	0.5	0.1
Q_0	19.6 $m^3 s^{-1}$	19.6 $m^3 s^{-1}$	39.3 $m^3 s^{-1}$	39.3 $m^3 s^{-1}$

and, if ξ is larger than about 10%,

$$\frac{B_{\max} - b}{b} \geq 1\% \tag{54}$$

7. Discussion

The model considers the laminar flow of magma in a volcanic conduit and processes occurring at some distance from the eruption vent: therefore, it can be applied to effusive or moderately explosive eruptions, as far as the laminar flow condition is fulfilled. We consider volcanic conduits with large values for the eccentricity ($\epsilon > 0.95$) and times following the beginning of the eruption, for which the temperature field can be considered stationary close to the conduit wall. We list in Table 1 the values of the fixed model parameters. In particular, we assume for the Dorn parameter and the activation energy values derived experimentally for basalts (e.g., Hartmann et al., 2014; Kirby & Kronenberg, 1987; Ranalli, 1995) and for the other parameters typical values for basaltic eruptions. From these values and the Arrhenius formula, close to the conduit wall, and for a distance in the order of magnitude of semi-minor axis, the medium viscosity is about 10^{13} Pa s, so that the Maxwell relaxation time τ_1 is in the order of 1000 s. In general, the pressure oscillation amplitude may vary during an eruption, for example due to pressure drop associated with magma chamber drainage (Gudmundsson et al., 2016). However, for the sake of simplicity, we consider a time interval in which p_0 can be assumed as constant.

As an example, Figures 4 and 5 show $B(t)$ and $Q(t)$ for some values of ϵ and τ_0 for fixed values of τ_1 ($\simeq$1000 s) and $Q_0 = 40$ $m^3 s^{-1}$ and the values of parameters are given in Table 1. The effect of viscoelastic rheology becomes remarkable for larger values of τ_0 and/or for eccentricity values closer to unity: when $\xi \geq 0.1$, the viscoelastic rheology entails that $B(t)$ ceases to oscillate symmetrically around the initial value as in elastic case, and, as ξ increases, $B(t)$ is almost always larger then b (Figure 4b). In addition, as the ratio τ_1/τ_0 decreases, $t_{\max}$ shifts from $\tau_0/4$ (elastic value) toward $\tau_0/2$, while $t_{\min}$ moves from 3/4 τ_0 toward τ_0.

In Table 2, we consider four cases corresponding to different choices of the conduit size and the period τ_0 of overpressure p: the initial value of the semi-minor axis b is fixed, while we select two different values for the initial semi-major axis a; the values of eccentricity ϵ range between 0.9992 and 0.9998 and τ_0 between 1 and 12 h, so that $\xi \geq 0.1$ and the effect of viscoelastic rheology can be appreciable. Table 2 includes the values of the parameter ξ and of the initial flow rate Q_0.For the values of Table 2, the semi-major axis $A(t)$ remains almost constant, while the semi-minor axis $B(t)$ varies as shown in Figure 6; the amplitudes of oscillations of $B(t)$ change from 2% and 9% with respect to the initial value b. Figure 6 shows the main effects due to the viscoelastic rheology with respect to elastic rheology (dotted curve): the increase in amplitude of oscillations of $B(t)$ and the time delay of its oscillation with respect to the elastic case. Because $A(t)$ is almost constant, $Q(t)$ shows the same behavior as $B(t)$ (Figure 7).

Figure 7 shows the flow rate Q as a function of time, for the cases of Table 2. The flow rate $Q(t)$ varies from 5% to 30% with respect to the initial value Q_0 (horizontal line). For values of τ_0 near to Maxwell time τ_1 ($\simeq$1,000 s), $Q(t)$ oscillates around the initial value Q_0 (case 4), as in the elastic rheology (dotted curve); for greater τ_0 (Cases 1–3) $Q(t)$ is almost always greater than the initial value Q_0, that is, it is above this value during most of the overpressure period τ_0. For the same value of τ_0 (Cases 2 and 3), the amplitude of flow rate oscillations increases with increasing eccentricity of the conduit. For a fixed eccentricity (Cases 1–2 and 3–4), the amplitude of flow rate oscillations increases with increasing values of τ_0. The times at which flow rate reaches its maximum and minimum values are delayed with respect to elastic case, as shown in 49 and 51.

During the 2018 eruption of Kīlauea Volcano, cyclic variations in effusion rate occurred at Fissure 8 on both short and long time scales (Neal et al., 2019; Patrick et al., 2019): multiparameter data showed that the short cycles, with period of 5–10 min, were driven by shallow outgassing, whereas longer cycles, with period of 1–2 days, were pressure-driven surges in magma supply triggered by summit caldera collapse events. For the short-time fluctuations, Patrick et al. (2019) estimated that lava velocity ranged between 4 and 15 m/s

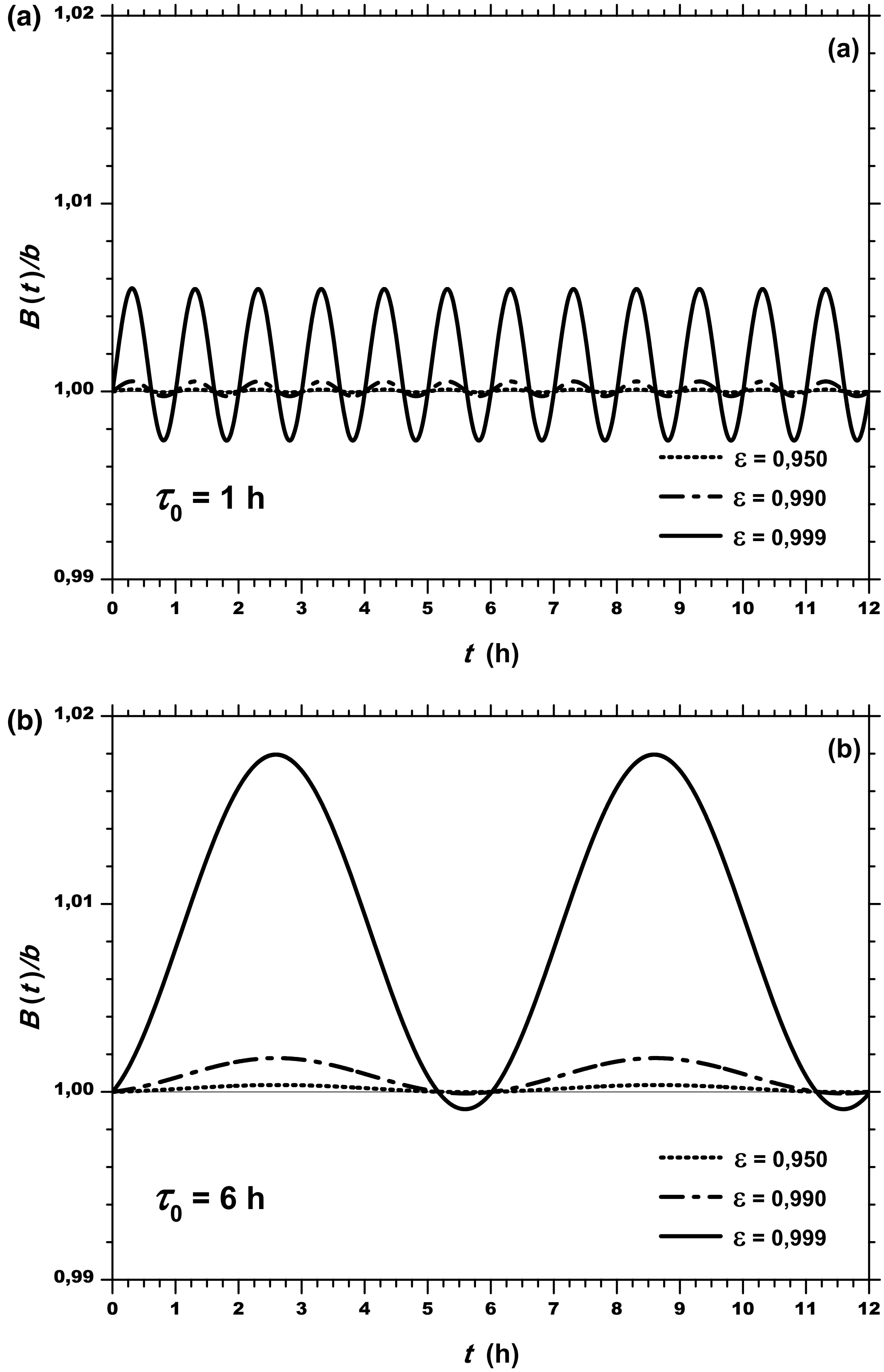

Figure 4. The semi-minor axis B as a function of time for different values of overpressure period τ_0 and conduit eccentricity ϵ, for a choice of values of parameters (Table 1) and $Q_0 = 40\ \mathrm{m^3\ s^{-1}}$

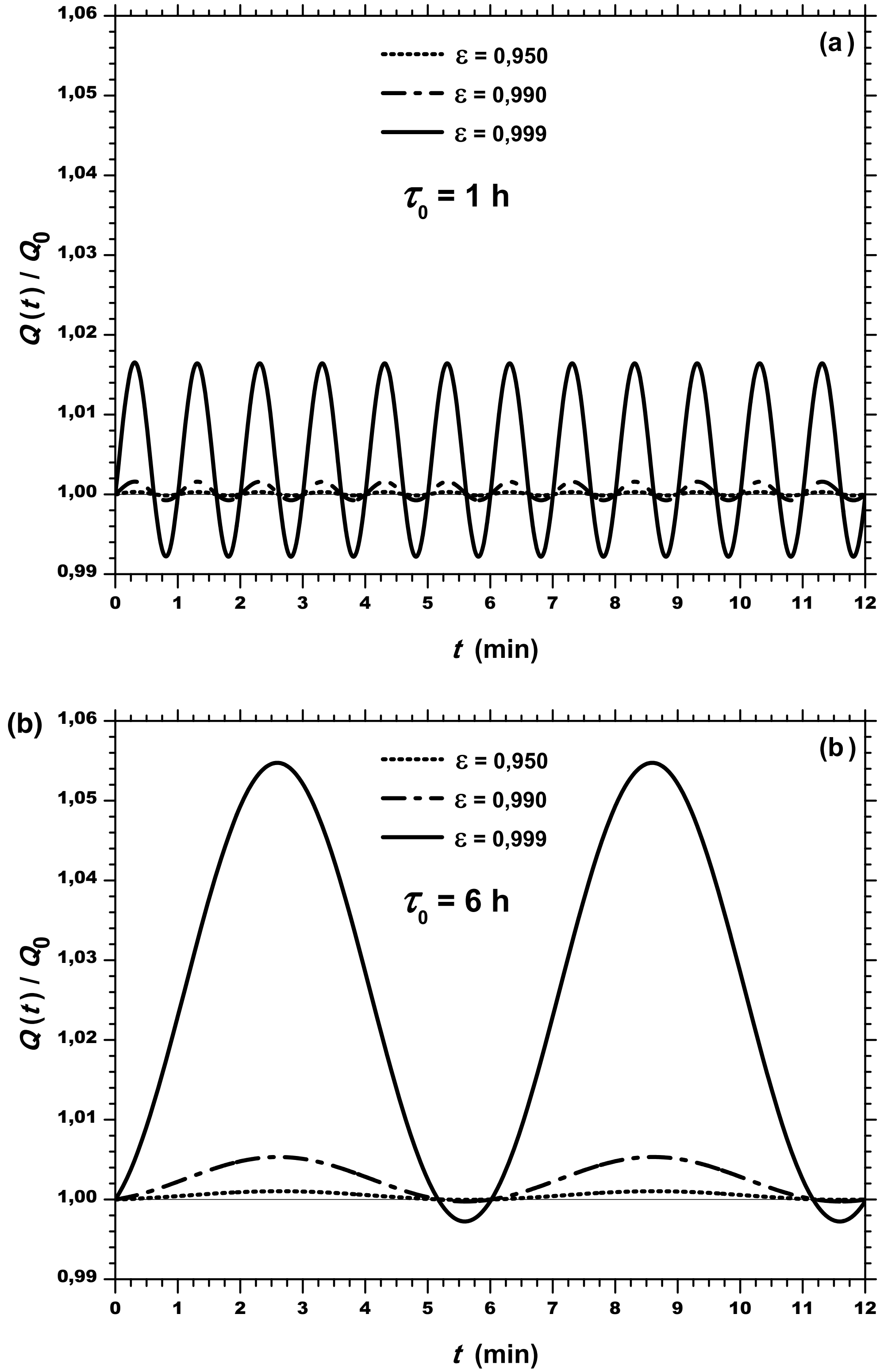

Figure 5. The flow rate Q as a function of time for different values of overpressure period τ_0 and conduit eccentricity ε, for a choice of values of parameters (Table 1) and $Q_0 = 40\ \mathrm{m^3\ s^{-1}}$

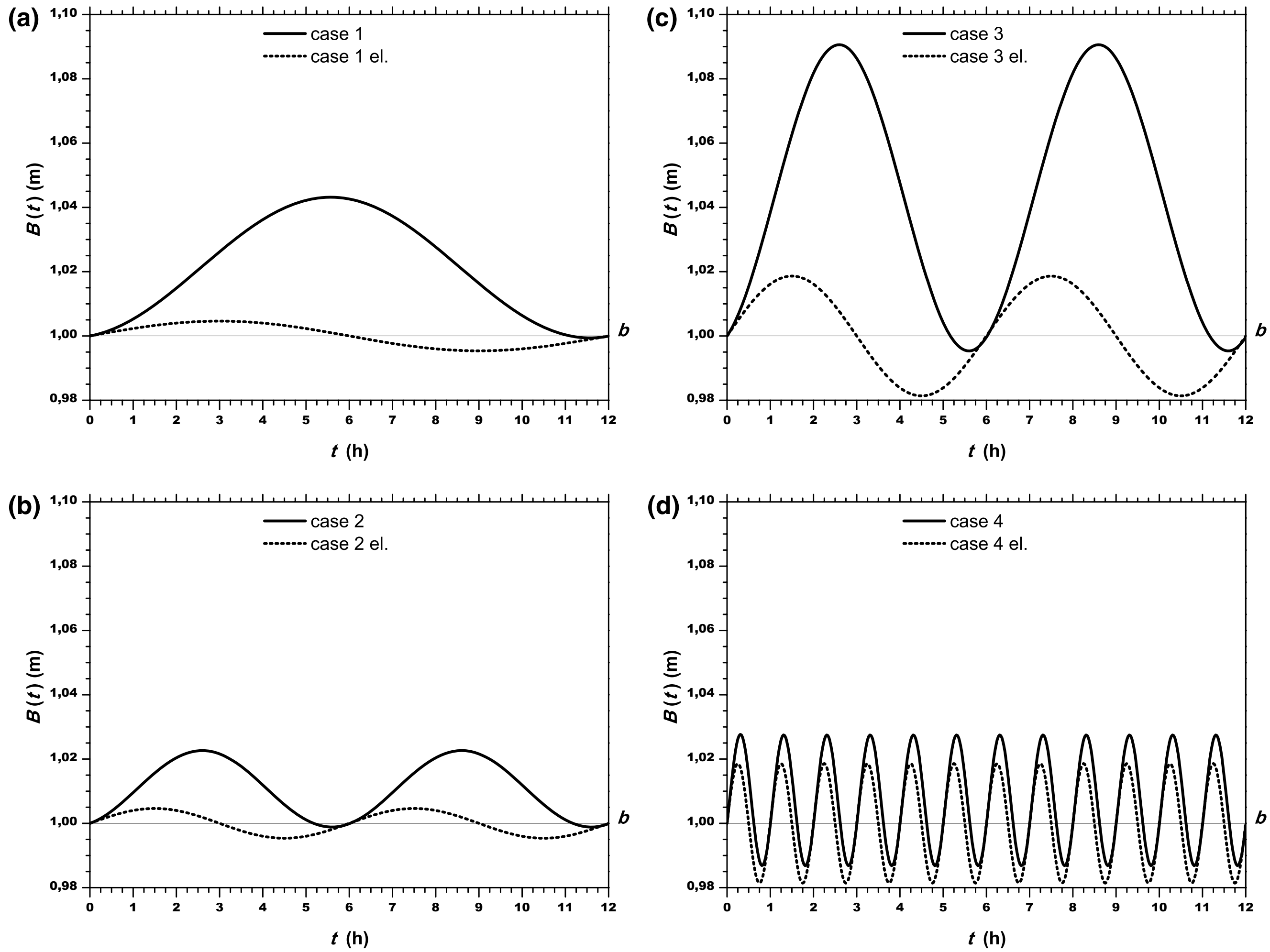

Figure 6. The semi-minor axis B as a function of time, for a choice of values of parameters (Table 1) and for the cases of Table 2: (a) case 1, (b) case 2, (c) case 3, and (d) case 4; dotted curves refer to a conduit embedded in an elastic medium

and effusion rate oscillated between 175 and 306 $m^3 s^{-1}$: these values implicate a low value of lava viscosity. We consider an elliptical eruptive fissure with semi-major axis $a \simeq 45$ m and semi-minor axis $b \simeq 0.5$ m ($\epsilon \simeq 0.9999$), and an overpressure with amplitude $p_0 = 10^5$ Pa and period $\tau_0 = 10$ min; in addition, we assume for the Dorn parameter $A_D \simeq 4.4 \times 10^9$ Pa s, for the lava viscosity $\eta_m \simeq 5$ Pa s, and for the body force intensity $\gamma \simeq 2 \times 10^2$ Pa m^{-1}. The semi-minor axis $B(t)$ varies as shown in Figure 8a; because $\xi \simeq 0.98$, the elastic case differs from the viscoelastic one. The flow rate oscillates between 185 and 315 m^3/s and $Q_0 \simeq 200$ $m^3 s^{-1}$ (Figure 8b); therefore, in the viscoelastic case, the pattern approximates the in-situ observations of short-time fluctuations of flow rate during the 2018 eruption of Kīlauea Volcano.

8. Conclusions

For an effusive eruption, we calculated the deformation of the volcanic conduit and the associated changes in flow rate due to short-term pressure oscillations. We considered an elliptical conduit embedded in a viscoelastic medium and assumed that the medium is a Maxwell body. We assumed that the deformation of the conduit is controlled by the viscosity of the region surrounding the conduit, which is assumed to be uniform. As a consequence of pressure oscillations, the semi axes of the conduit are quasi periodic functions of time with the same period as pressure.

For fissures, the viscoelastic rheology entails an increase in oscillation amplitude with respect to the elastic case. This effect is due to the viscoelastic rheology of the medium surrounding the volcanic conduit and

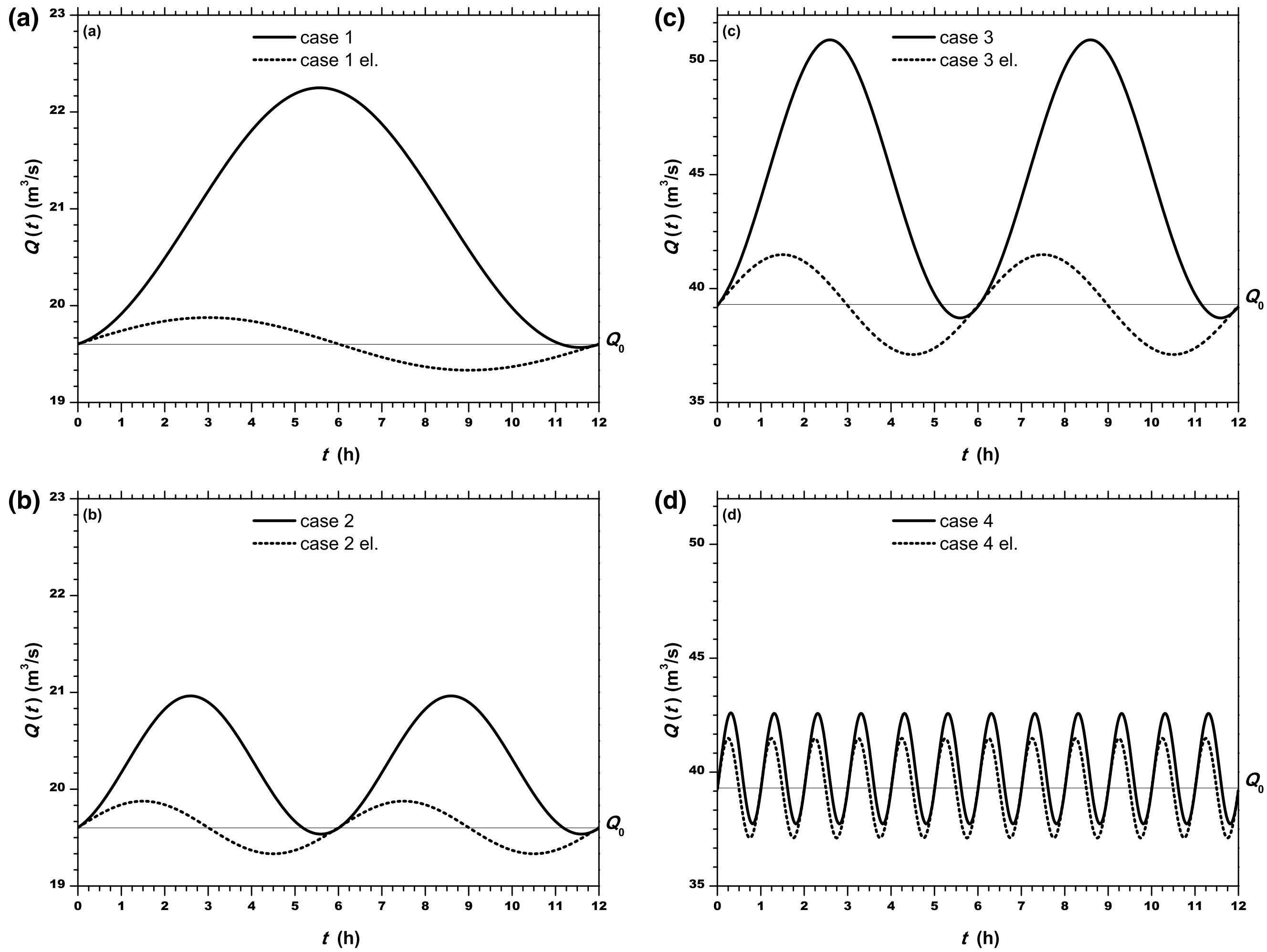

Figure 7. Flow rate Q as a function of time, for a choice of values of parameters (Tables 1 and 2): (a) case 1, (b) case 2, (c) case 3, and (d) case 4; dotted curves refer to a conduit embedded in an elastic medium. Graphs in (a and b) and (c and d) use two different scales.

becomes remarkable for larger values of the ratio between overpressure period and Maxwell time and/or for eccentricity value closer to unity, for a given value of pressure oscillation amplitude.

For values of the period of pressure oscillation near to Maxwell time, flow rate oscillates around its initial value, as in the elastic case; for larger period values, flow rate is almost always larger than its initial value and oscillates around a higher value than initial one. For a given overpressure period, the amplitude of flow rate oscillations increases with increasing eccentricity of the conduit. For a fixed eccentricity, the amplitude of flow rate oscillation increases with increasing values of the period of pressure oscillation. The flow rate can vary from 5% to 30% with respect to the initial value. The viscoelastic rheology entails a time delay in flow rate oscillation with respect to overpressure oscillation; this delay depends on ratio between overpressure period and Maxwell time.

In conclusion, the effect of viscoelastic rheology is to produce significant flow rate oscillations also in conduits with smaller eccentricities with respect to the elastic case; moreover, viscoelastic rheology allows to achieve higher (average) flux rates with lower overpressures.

The model provides a possible explanation of observed changes in the effusion rate during effusive eruptions occurring on timescales less than the total duration of eruption. This pulsatory style can have a different period with respect the overpressure period that causes it. The model can approximate the in situ observations of short-time fluctuations of flow rate during the 2018 eruption of Kīlauea Volcano.

10.1029/2020JB020642

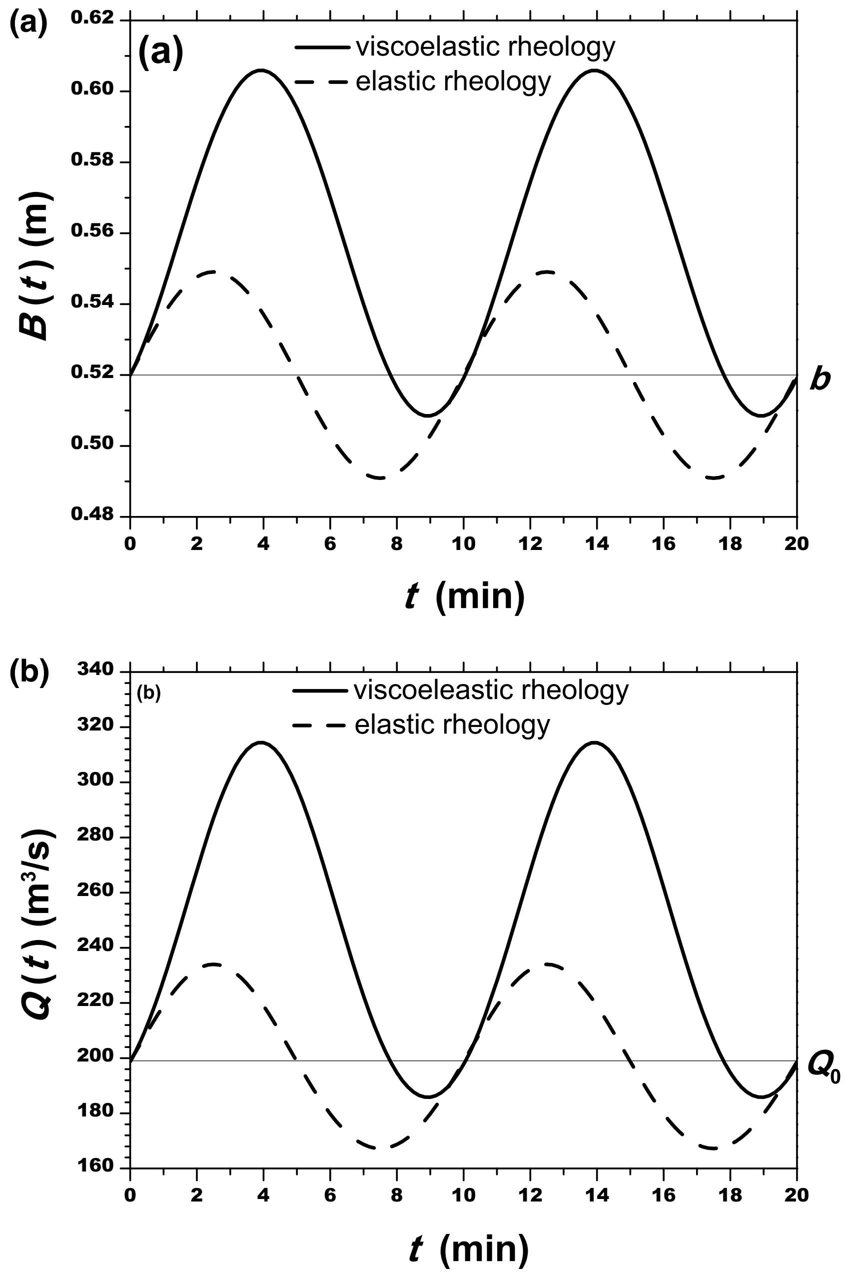

Figure 8. The semi-minor axis B (a) and flow rate Q (b) as functions of time, obtained from the model in the elastic and viscoelastic cases, using the data of flow oscillations rate during the 2018 eruption of Kīlauea Volcano (Patrick et al., 2019)

Data Availability Statement

This paper is a theoretical work and does not contain new data.

Acknowledgments
The authors are grateful to the Editor André Revil, the Associate Editor Mike Poland, and two anonymous reviewers for useful comments and suggestions on the first version of the paper.

References

Bonafede, M., Dragoni, M., & Quareni, F. (1986). Displacement and stress fields produced by a centre of dilation and by a pressure source in a viscoelastic half-space: Application to the study of ground deformation and seismic activity at Campi Flegrei, Italy. *Geophysical Journal International*, *87*(2), 455–485. https://doi.org/10.1111/j.1365-246X.1986.tb06632.x

Calvari, S., & Pinkerton, H. (1999). Lava tube morphology on Etna and evidence for lava flow emplacement mechanisms. *Journal of Volcanology and Geothermal Research*, *90*(3), 263–280. doi:https://doi.org/10.1016/S0377-0273(99)00024-4

Christensen, R. (1982). *Theory of viscoelasticity* (2nd ed.). New York, NY: Academic Press.

Del Negro, C., Cappello, A., Neri, M., Bilotta, G., Hérault, A., & Ganci, G. (2013). Lava flow hazards at Mount Etna: Constraints imposed by eruptive history and numerical simulations. *Scientific Reports*, *3*(1), 3493–3493. https://doi.org/10.1038/srep03493

Dragoni, M., D'Onza, F., & Tallarico, A. (2002). Temperature distribution inside and around a lava tube. *Journal of Volcanology and Geothermal Research*, *115*(1), 43–51. doi:https://doi.org/10.1016/S0377-0273(01)00308-0

Dragoni, M., & Magnanensi, C. (1989). Displacement and stress produced by a pressurized, spherical magma chamber, surrounded by a viscoelastic shell. *Physics of the Earth and Planetary Interiors*, *56*(3), 316–328. doi:https://doi.org/10.1016/0031-9201(89)90166-0

Dragoni, M., & Santini, S. (2007). Lava flow in tubes with elliptical cross sections. *Journal of Volcanology and Geothermal Research*, *160*(3), 239–248. doi:https://doi.org/10.1016/j.jvolgeores.2006.09.008

Dragoni, M., & Tallarico, A. (2008). Temperature field and heat flow around an elliptical lava tube. *Journal of Volcanology and Geothermal Research*, *169*(3), 145–153. doi:https://doi.org/10.1016/j.jvolgeores.2007.08.016

Dragoni, M., & Tallarico, A. (2019). Changes in lava effusion rate from a volcanic fissure due to pressure changes in the conduit. *Geophysical Journal International*, *216*(1), 692–702. https://doi.org/10.1093/gji/ggy454

Filippucci, M., Tallarico, A., & Dragoni, M. (2013). Simulation of lava flows with power-law rheology. *Discrete and Continuous Dynamical Systems – Series S*, *6*(3), 677–685. https://doi.org/10.3934/dcdss.2013.6.677

Folch, A., Fernández, J., Rundle, J., & Martí, J. (2000). Ground deformation in a viscoelastic medium composed of a layer overlying a half-space: A comparison between point and extended sources. *Geophysical Journal International*, *140*(1), 37–50. https://doi.org/10.1046/j.1365-246X.2000.00003.x

Fung, Y. (1965). *Foundations of solid mechanics*. Englewood Cliffs, NJ: Prentice-Hall.

Gonnermann, H. M., & Manga, M. (2013). Dynamics of magma ascent in the volcanic conduit. In R. Lopes, S. A. Fagents, T. K. P. Gregg (Ed.), *Modeling volcanic processes: The physics and mathematics of volcanism*. Cambridge, MA: Cambridge University Press.

Gudmundsson, M., Jónsdóttir, K., Hooper, A., Holohan, E., Halldórsson, S., Ófeigsson, B., et al. (2016). Gradual caldera collapse at Bárdarbunga volcano, Iceland, regulated by lateral magma outflow. *Science*, *353*(6296), aaf8988-1–aaf8988-8. https://doi.org/10.1126/science.aaf8988

Hartmann, J., Moosdorf, N., Lauerwald, R., Hinderer, M., & West, A. J. (2014). Global chemical weathering and associated P-release—The role of lithology, temperature and soil properties. *Chemical Geology*, *363*, 145–163. doi:https://doi.org/10.1016/j.chemgeo.2013.10.025

Ida, Y. (1996). Cyclic fluid effusion accompanied by pressure change: Implication for volcanic eruptions and tremor. *Geophysical Research Letters*, *23*(12), 1457–1460. https://doi.org/10.1029/96GL01325

Jellinek, A. M., & Bercovici, D. (2011). Seismic tremors and magma wagging during explosive volcanism. *Nature*, *470*(7335), 522–525. https://doi.org/10.1038/nature09828

Ji, S., Sun, S., Wang, Q., & Marcotte, D. (2010). Lamé parameters of common rocks in the Earth's crust and upper mantle. *Journal of Geophysical Research*, *115*, B06314. https://doi.org/10.1029/2009JB007134

Kirby, S. H., & Kronenberg, A. K. (1987). Rheology of the lithosphere: Selected topics. *Reviews of Geophysics*, *25*(6), 1219–1244. https://doi.org/10.1029/RG025i006p01219

Landau, L. D., & Lifshits, E. M. (1970). *Theory of elasticity* (2nd ed.), Pergamon Press.

Lautze, N. C., Harris, A. J., Bailey, J. E., Ripepe, M., Calvari, S., Dehn, J., et al. (2004). Pulsed lava effusion at Mount Etna during 2001. *Journal of Volcanology and Geothermal Research*, *137*(1), 231–246. doi:https://doi.org/10.1016/j.jvolgeores.2004.05.018

Neal, C., Brantley, S., Antolik, L., Babb, J., Burgess, M., Calles, K., et al. (2019). Volcanology: The 2018 rift eruption and summit collapse of Kīlauea Volcano. *Science*, *363*(6425), 367–374. https://doi.org/10.1126/science.aav7046

Newman, A., Dixon, T., Ofoegbu, G., & Dixon, J. (2001). Geodetic and seismic constraints on recent activity at Long Valley Caldera, California: Evidence for viscoelastic rheology. *Journal of Volcanology and Geothermal Research*, *105*(3), 183–206. doi:https://doi.org/10.1016/S0377-0273(00)00255-9

Patrick, M., Dietterich, H., Lyons, J., Diefenbach, A., Parcheta, C., Anderson, K., et al. (2019). Cyclic lava effusion during the 2018 eruption of Kīlauea Volcano. *Science*, *366*(6470), 1–10. https://doi.org/10.1126/science.aay9070

Peltier, W. R. (1974). The impulse response of a Maxwell Earth. *Reviews of Geophysics*, *12*(4), 649–669. doi: https://doi.org/10.1029/RG012i004p00649

Piombo, A., Tallarico, A., & Dragoni, M. (2007). Displacement, strain and stress fields due to shear and tensile dislocations in a viscoelastic half-space. *Geophysical Journal International*, *170*(3), 1399–1417. https://doi.org/10.1111/j.1365-246X.2007.03283.x

Piombo, A., Tallarico, A., & Dragoni, M. (2016). Role of mechanical erosion in controlling the effusion rate of basaltic eruptions. *Geophysical Research Letters*, *43*(17), 8970–8977. https://doi.org/10.1002/2016GL069737

Ranalli, G. (1995). *Rheology of the Earth*. London: Chapman and Hall.

Ripepe, M., Harris, A. J., & Carniel, R. (2002). Thermal, seismic and infrasonic evidences of variable degassing rates at Stromboli volcano. *Journal of Volcanology and Geothermal Research*, *118*(3), 285–297. doi: https://doi.org/10.1016/S0377-0273(02)00298-6

Sakimoto, S. E. H., & Zuber, M. T. (1998). Flow and convective cooling in lava tubes. *Journal of Geophysical Research*, *103*(B11), 27465–27487. https://doi.org/10.1029/97JB03108

Sparks, R. S. J. (2003). Dynamics of magma degassing. *Geological Society, London, Special Publications*, *213*(1), 5–22. https://doi.org/10.1144/gsl.sp.2003.213.01.02

Tallarico, A., Dragoni, M., Filippucci, M., Piombo, A., Santini, S., & Valerio, A. (2011). Cooling of a channeled lava flow with non-Newtonian rheology: Crust formation and surface radiance. *Annals of Geophysics*, *54*(5), 510–520. https://doi.org/10.4401/ag-5335

Vicari, A., Ganci, G., Behncke, B., Cappello, A., Neri, M., & Del Negro, C. (2011). Near-real-time forecasting of lava flow hazards during the 12–13 January 2011 Etna eruption. *Geophysical Research Letters*, *38*(13), 1–7. https://doi.org/10.1029/2011GL047545

Voight, B., Sparks, R., Miller, A., Stewart, R., Hoblitt, R., Clarke, A., et al. (1999). Magma flow instability and cyclic activity at Soufriere Hills volcano, Montserrat, British West Indies. *Science*, *283*(5405), 1138–1142. https://doi.org/10.1126/science.283.5405.1138

Wadge, G. (1981). The variation of magma discharge during basaltic eruptions. *Journal of Volcanology and Geothermal Research*, *11*(2), 139–168. doi: https://doi.org/10.1016/0377-0273(81)90020-2

Whitehead, J. A., & Helfrich, K. R. (1991). Instability of flow with temperature-dependent viscosity: A model of magma dynamics. *Journal of Geophysical Research*, *96*(B3), 4145–4155. https://doi.org/10.1029/90JB02342

Woods, A., & Koyaguchi, T. (1994). Transitions between explosive and effusive eruptions of silicic magmas. *Nature*, *370*(6491), 641–644. https://doi.org/10.1038/370641a0

Wylie, J. J., Voight, B., & Whitehead, J. A. (1999). Instability of magma flow from volatile-dependent viscosity. *Science*, *285*(5435), 1883–1885. https://doi.org/10.1126/science.285.5435.1883